Published in final edited form as:
Biofabrication. 2014 September ; 6(3): 035026. doi:10.1088/1758-5082/6/3/035026.

Sensory Axon Guidance with Semaphorin 6A and Nerve Growth Factor in a Biomimetic Choice Point Model

J. Lowry Curley, **Gary C. Catig**, **Elaine L. Horn-Ranney**, and **Michael J. Moore***
Lindy Boggs Bldg., Suite 500, Department of Biomedical Engineering, Tulane University, New Orleans, LA 70118, USA

J. Lowry Curley: jcurley@tulane.edu; Gary C. Catig: catig@tulane.edu; Elaine L. Horn-Ranney: ehorn1@tulane.edu

Abstract

The direct effect of guidance cues on developing and regenerating axons *in vivo* is not fully understood, as the process involves a multiplicity of attractive and repulsive signals, presented both as soluble and membrane-bound ligands. A better understanding of axon guidance is critical to functional recovery following injury to the nervous system through improved outgrowth and mapping of damaged nerves. Due to their implications as inhibitors to CNS regeneration, we investigated the repulsive properties of Semaphorin 6A and Ephrin-B3 on E15 rat dorsal root ganglion explants, as well as possible interactions with soluble gradients of chemoattractive nerve growth factor. We employed a 3D biomimetic *in vitro* choice point model, which enabled the simple and rapid preparation of patterned gel growth matrices with quantifiable presentation of guidance cues in a specifiable manner that resembles the *in vivo* presentation of soluble and/or immobilized ligands. Neurites demonstrated an inhibitory response to immobilized Sema6A by lumbosacral DRG explants, while no such repulsion was observed for immobilized Ephrin-B3 by explants at any spinal level. Interestingly, Sema6A inhibition could be partially attenuated in a concentration-dependent manner through the simultaneous presentation of soluble NGF gradients. The *in vitro* model described herein represents a versatile and valuable investigative tool in the quest for understanding developmental processes and improving regeneration following nervous system injury.

1. Introduction

Through secreted and bound guidance cues, developing and regenerating axons navigate a complex environment in order to reach their targets. Often along their paths *in vivo*, the axonal growth cones encounter choice points regulated by the synchronized effect of numerous receptor-ligand interactions. The molecular guideposts governing these choice points are multifaceted, including bound cell adhesion molecules and soluble and immobilized chemoattractive and chemorepulsive signals (McCormick and Leipzig, 2012). The same cues mediating neuronal axon development are thought to be important for functional recovery following traumatic injury. Strategies to promote functional regeneration will need to supply a permissive environment for maximal axonal outgrowth (Schmidt and Leach, 2003), and just as importantly, may need to facilitate mapping of

*Corresponding Author: Michael J. Moore, Ph.D., Phone: 504-865-5897; Fax: 504-862-8779; mooremj@tulane.edu.

growth to proper physiological connections (Harel and Strittmatter, 2006; Moore and Goldberg, 2010). A greater understanding of the interplay between attractive and repulsive cues will thus be required both for describing developmental processes and devising treatments.

One of these important guidance molecules, Semaphorin 6A (Sema6A) is a transmembrane ligand with direct applications to developmental pathfinding in axons of the corticospinal tract (Runker et al., 2008), sympathetic ganglion (Suto et al., 2005), and sensory dorsal root ganglion (DRG) (Mauti et al., 2007). It has also been shown to be highly expressed in adult oligodendrocytes, establishing it as part of the inhibitory environment consequent to CNS damage (Shim et al., 2012). Similarly, Ephrin-B3 is a glial-expressed transmembrane ligand that regulates guidance in the corticospinal tract (Yokoyama et al., 2001) and mediates axon pruning (Xu and Henkemeyer, 2009), and has likewise been implicated as a myelin-based inhibitor of regeneration (Benson et al., 2005). In contrast, we are not aware of any reports of Ephrin-B3 inhibiting growth from sensory DRG explants.

Nerve growth factor (NGF) is a well-characterized survival and trophic factor expressed in many parts of the nervous system and target organs (Sofroniew et al., 2001). In addition to its well-established functions during development, it has also demonstrated regenerative properties following trauma, both through up-regulation of outgrowth and down-regulation of chemorepulsive cues (Romero et al., 2001; Tang et al., 2007; Wood et al., 2010). NGF has been shown to influence the effects of the semaphorin family, specifically Sema3A, whose repulsive effects were mediated by changes in NGF concentration (Ben-Zvi et al., 2008; Dontchev and Letourneau, 2002).

Potentially nuancing some of these findings is that although Sema6A and Ephrin-B3 are both naturally expressed as membrane bound ligands, they have most often been studied as soluble dimers. Similarly, the trophic effects of NGF have often been investigated by changing uniform concentration, even though secretion by cells in specific anatomic locations necessarily results in concentration gradients. Further, it is not entirely clear to what extent single-molecule experiments at the microscale of the growth cone are predictive of macroscale guidance of cell populations responding to multiple cues *in vivo*. Finally, neurons are increasingly being observed to display more physiologically-realistic behavior when cultured in 3D matrices, as compared to surface-plated preparations (Desai et al., 2006; Irons et al., 2008; Lai et al., 2012).

A number of *in vitro* model systems have been developed for the study of neurite guidance cues, a growing field which has been reviewed in detail recently (Roy et al., 2013). Our focus was to demonstrate the utility of a biomimetic preparation capable of presenting multiple guidance cues, whether in soluble or immobilized configurations, within a 3D matrix. We observed DRG neurite responses to immobilized Sema6A and Ephrin-B3 and sought to investigate the interactive effects of soluble NGF. We employed a micropatterned hydrogel choice point model, based on previous work (Curley and Moore, 2011; Horn-Ranney et al., 2013), allowing for the simple, quantifiable presentation of individual or multiple guidance cues in a controlled specifiable manner characterized by structurally confined, biomimetic, 3D neurite extension and highly reproducible growth conditions.

2. Materials and methods

2.1. Biomimetic in vitro DRG explant culture environment

The dual hydrogel environment used for tissue explant culture has been previously described (Curley et al., 2011; Curley and Moore, 2011). The fabrication process is summarized in Fig. 1 and described below. Using a digital micro-mirror device (DMD, Discovery™ 3000, Texas Instruments, Dallas, TX) as a dynamic photomask, the black and white mask of interest (Fig. 2 A, Fig. 3 A), was loaded through a graphical user interface. An inverted microscope mounted underneath the DMD was used to visualize and align the photomask. Next, a 500 μL volume of 10% w/v polyethylene glycol (PEG, MW 1000,Polysciences Inc., Warrington, PA) and .5% Irgacure 2959 (Ciba Specialty Chemicals, Basel, Switzerland) in DPBS (Invitrogen, Grand Island, NY) was added to permeable cell culture inserts (Corning Inc., Corning, NY) and crosslinked with a UV light source (OmniCure 1000 with 320–500 nm filter, EXFO, Quebec, Canada)at 181 mW/cm^2 for ~55 seconds, creating a cell restrictive border. The thickness of the PEG gel (previously reported as ~480 μm using the conditions described, Curley and Moore, 2011) may be controlled through the initial volume of PEG solution added.

Following three washes in sterile conditions with DPBS containing 1% penicillin/ streptomycin (Invitrogen), a 1% α-carboxy-2-nitrobenzyl cysteine agarose (CNBC-agarose) in DPBS (Invitrogen, Grand Island, NY) supplemented with 1 μg/mL laminin was added as a cell permissive region. After the CNBC-agarose was introduced, 1.5 mL prechilled DPBS was added inside each 6-well culture plate followed by refrigeration at 4° C for 15 minutes. Depth of the cell permissive CNBC-agarose (previously reported as ~470 μm, Horn-Ranney et al., 2013) is dependent on the thickness of PEG and can be thusly modified. Additionally, the size and geometry of each mask can also be easily adjusted to match different explant sizes, even at the last minute, using any image manipulation program.

Protein micropatterning techniques have also been reported in depth(Horn-Ranney et al., 2013), but will be detailed again below. CNBC-agarose was synthesized as previously reported to incorporate photo-caged thiol side groups capable of spatial protein patterning in the cell permissive gel (Horn-Ranney et al., 2013). For lower concentrations of bound Sema6A, a 1% solution of CNBC-agarose was mixed with a 1% solution of unmodified type IX-A agarose (Sigma-Aldrich, St. Louis, MO) at 10% prior to gelation.

2.2. Protein modification

Semaphorin 6A Fc chimera (Sema6A), Ephrin-B3 Fc chimera (Ephrin-B3) and bovine serum albumin (BSA), were prepared for covalent immobilization to a CNBC-agarose hydrogel by modifying each protein with a maleimide group for immobilization and a fluorescent tag for visualization(Rahman et al., 2010). A sulfo-SMCC with cyclohexane spacer (Thermo Scientific, Rockford, IL) was used simultaneously with an Alexa Fluor 488 labeling kit (Molecular Probes, Eugene, OR). Sema 6A, Ephrin-B3 (R & D Systems, Minneapolis, MN) and gel filtration quality BSA (Sigma-Aldrich) were reconstituted at 0.4 mg/mL, followed by the addition of 134 nM of fluorescent dye/nM protein and 146 nM sulfo-SMCC/nM protein, and the solution was allowed to react for 15 minutes at 4°C. The

ratios of fluorescent dye and sulfo- SMCC per nM protein may have to be adjusted for optimal binding of different proteins. Finally, excess crosslinker and reactive dye were removed using a fluorescent dye removal column (Thermo Scientific) as directed. A BCA assay kit (Thermo Scientific) was used to determine protein concentration following conjugation. In order to quantify the amount of bound protein, a standard curve was determined using known concentrations of each protein dissolved in agarose gel inside PEG gel molds with identical thickness to those used in experiments.

Fluorescent NGF was prepared for soluble experiments in order to visualize protein diffusion. NGF (Invitrogen) was tagged using an NHS-Fluorescein labeling kit (Thermo Scientific), as directed. Again, excess reagents were removed using dye removal columns, and a NanoOrange Protein Quantification Kit (Invitrogen) was used to determine final concentrations. Finally, a standard curve in identical conditions was again used to ascertain experimental concentrations of NGF temporally.

2.3. Neurite avoidance experiments with immobilized proteins

Subsequently, regions of the CNBC-agarose gel specified for protein binding were irradiated with 90 s of UV light patterned with a new photomask (Fig. 2 B), exposing free thiols for the binding of maleimide groups(Horn-Ranney et al., 2013). Irradiated gels were then blocked with 5% BSA (Invitrogen) at 4°C for 1 hour, incubated in maleimide-conjugated protein (either BSA, Sema6A or Ephrin-B3) solution (5 ug/mL) at 4°C for 48 hours, then washed in 2% BSA, 0.1% Tween 20 (Sigma-Aldrich) in DPBS for 5 days at 4°C with one solution change per day, all at 4°C. Time between irradiation of CNBC-agarose and protein binding should be minimized, as exposed thiol availability for maleimide binding decreases with time due to oxidation.

All procedures involving animals were approved by the Institutional Animal Care and Use Committee (IACUC) in accordance with federal guidelines. Prior to the incorporation of tissue explants, gels were incubated in growth media overnight at 37°C and 5% CO_2, with two subsequent media changes. Embryonic day 15 (E15) dorsal root ganglion (DRG) were dissected from Long Evans rats, and sorted by spinal level into lumbosacral, thoracic and cervicothoracic regions. DRG explants were inserted within the circular regions of the agarose gels, ensuring that each DRG explant was placed within the depth of the gel, after the protein immobilization steps were carried out. Each DRG explant was carefully placed directly on top of the CNBC-agarose and then gently pressed into the gel using dull forceps. Explants were cultured in Neurobasal medium with 2% B-27 supplement, 1% penicillin/ streptomycin, 0.5 mM L-glutamine and 5 or 20 ng/mL NGF (Invitrogen) at 37°C and 5% CO_2 with media changes every 48 hours. DRG neurite growth was monitored under brightfield microscopy, and each construct was fixed when growth reached the end of either channel, approximately 9 – 12 days. We chose the unifying metric of length, versus a time endpoint, due to the different rates of neurite growth for 5 and 20 ng/mL NGF.. Constructs were fixed in 4% paraformaldehyde at 37°C for two hours.

2.4. Neurite outgrowth experiments with immobilized proteins and soluble protein gradients

The dual hydrogel constructs were created as described above, but using an alternative photomask to include circular wells at the ends of the channels in order to form the diffusible gradients (Fig. 3 A). The permissive gel, 1% CNBC-A, was added to the void and bound molecules were again added in distinct regions (Fig. 3 B). Immediately after the addition of DRG explants, simultaneous gradients of NGF and casein (Invitrogen, as a control) were introduced to the agarose gel by adding the respective solution to the empty well at the end of opposite channels. In order to maintain a gradient with an average absolute concentration on the order of 1.0 nM (Rosoff et al., 2004), both NGF and casein were added to the wells at a concentration of 40 nM each, with fresh protein solution added every 3 hours. A previously-reported, validated diffusion model, using experimentally determined diffusion coefficients of 31.2 μm2/s for PEG gel and 107.4 μm2/s for agarose gel, was used to simulate diffusion behavior in the dual hydrogel constructs (Horn-Ranney et al., 2013). Diffusion experiments in the configuration employed for neurite outgrowth experiments were performed for further validation, and computational simulations were used to determine the concentration and frequency with which protein sources were replenished.

Only lumbosacral explants were used in NGF gradient experiments. For NGF gradient experiments, growth medium was identical except no NGF was used in the medium, which was changed every 24 hours. For NGF gradient experiments, all samples were fixed when growth reached the end of either channel in any one construct, approximately 72 hours. Constructs were again fixed in 4% paraformaldehyde at 37°C for two hours.

2.5. Immunocytochemistry

Neurite staining was performed using mouse monoclonal [2G10] to neuron specific β III tubulin primary antibody and goat-anti-mouse IgG- H&L (CY3.5) secondary antibody (AbCam, Cambridge, MA). Receptor staining was done with rabbit polyclonal anti-Plexin A4 primary antibody or rabbit polyclonal anti-Eph receptor A4 primary antibody and donkey anti-rabbit (Dylight 488) IgG- H&L secondary antibody (AbCam). Blocking was performed for one hour with 5% BSA in PBS for the primary antibody and 5% goat or donkey serum for the secondary antibody. Primary and secondary staining was carried out in PBS with 0.1% Saponin and 2% BSA for 48 hours, followed by three washes in PBS with 0.1% Saponin. Image acquisition used a Nikon AZ100 stereo zoom microscope (Nikon, Melville, NY) for conventional fluorescence and a Zeiss LSM 510 Meta microscope (Zeiss, Oberkocken, Germany) for confocal fluorescence. Image J (National Institutes of Health, Bethesda, MD) was used for post processing of images.

2.6. Immunofluorescence quantification and analysis

Confocal imaging of β III tubulin stained neurites in both channels was performed throughout the depth of the constructs. Maximum intensity Z-stacks were obtained from the confocal images of each channel. In order to quantify neurite growth, automatic thresholding (mean) was used, followed by pixel volume analysis for each channel. Channels which were too long to image in one stack were stitched together after thresholding. The area measured for volume analysis was 601 μm in length by 531 μm in width for neurite avoidance

experiments and 1151μm × 909μm for neurite outgrowth experiments. During immunofluorescence quantification and analysis, it became apparent that the universal presence of a large number of neurites at the hydrogel border produced a large amount of error as it tended to normalize results across conditions (data not shown). For this reason, we methodically used a universal region of interest (ROI) which included only the bulk agarose and excluded the border region in every channel (Fig. 2 C). This allowed us to mitigate any error which the counting of neurites not inside the growth permissive gel would have introduced. For avoidance experiments, channels were characterized as being towards the bound protein (Sema6A, Ephrin-B3 or BSA) or away from bound protein. In outgrowth experiments, growth was identified as towards the soluble gradient of NGF or towards the soluble gradient of casein. A guidance ratio (Rosoff et al., 2004) was used to determine what effect immobilized or soluble proteins had on growth:

$$Guidance\ ratio_{toward\ bound\ protein} = \frac{\%toward\ protein - \%away\ from\ protein}{100\%} \quad (1)$$

$$Guidance\ ratio_{towardNGFgradient} = \frac{\%towardNGF - \%away\ fromNGF}{100\%} \quad (2)$$

Using these guidance ratio equations, a positive number was indicative of a chemoattractive response, while a negative value represented chemorepulsion. DRG explants showing no growth into either channel were excluded from analyses (approximately 10% of explants plated).

Expression of both Plexin A4 and EphA4 was analyzed separately using fluorescent images taken using identical conjugated secondary antibodies as well as with identical gain, offset and exposure times in order to minimize differences due merely to staining and image acquisition methods. DRG explant boundaries were traced manually, and the mean fluorescence was determined inside of the DRG as well as outside (background). The average of the background subtracted from the receptor fluorescence value was calculated between DRG spinal levels, and this semi-quantitative method allowed for the comparison of relative fluorescence between DRG types.

2.7. Statistical analysis

For immobilized proteins, data was grouped according to DRG explant location (lumbosacral, thoracic or cervicothoracic) and type of bound protein (Sema6A, Ephrin-B3 or BSA). In order to establish significance between conditions involving two groups, a two tailed student's t-test of equal variance ($p<0.05$) was used. Equality of variance was calculated using Levene's test ($p<0.05$). To test for differences between conditions containing three or more groups, Minitab (Minitab, State College, PA) was used to perform one-way ANOVA separately followed by Games-Howell post-hoc analysis ($p < 0.05$). Unless otherwise specified, data are presented as mean ± standard deviation.

3. Results

3.1. Quantification of immobilized and soluble concentration profiles

It was important that concentrations of immobilized and soluble ligands could be quantifiable as presented to neurites extending into the cell permissive regions of the gels. Sema6A-Fc was covalently immobilized in a specific region of a micropatterned agarose gel (Fig. 2 A–C) and found to be present at a concentration of 146 ± 27nM (Fig. 2 D). BSA was similarly immobilized in the gel as a control and found to be bound at a concentration of 275 ± 34 nM. Protein fluorescence was assessed both immediately after protein binding and following fixation at the conclusion of the study, and no significant differences were detected (data not shown). Florescence of bound protein was significantly higher ($p < 0.001$) than background agarose fluorescence for all proteins (Fig. 2 D).

A computational model of diffusion in dual hydrogel systems had previously been validated using diffusion experiments with fluorescent proteins (Horn-Ranney et al., 2013). This same diffusion model was validated with diffusion experiments matching the specific geometries used in the present study (Fig. 3 A–C), and used to determine the initial concentration and frequency of addition of an NGF solution to a reservoir distal from the DRG. Experimental and simulated concentration profiles are shown in Fig. 3 D–F. The percent error between the computational model and experimental data was calculated to be 18.9%, 1.8% and 7.7% error for 15, 60 and 180 minutes, respectively. After adding a 40nM solution, the concentration profile within the agarose growth region was confirmed to form as an exponentially-decaying gradient which resolved to an approximately linear gradient within the first several minutes (Fig. 3 E). After one hour of passive diffusion, the gradient was linear with a slope of approximately 0.001 nM/μm and average concentration of roughly 1.5 nM (Fig. 3 D). The concentration profile gradually dissipated to a negligible gradient by three hours, though the baseline concentration remained within the previously reported physiologically relevant range (Rosoff et al., 2004). Because of the exponential nature of the gradient immediately following introduction, we previously determined that linearity was maintained more effectively by letting the gradient disappear prior to repeated additions (Horn-Ranney et al., 2013). The concentration gradient manifesting in the opposite channel was minimal and in the opposite orientation, as expected (Fig. 3 F). From these simulations and experiments, it was determined that solutions would be added to the reservoirs every three hours.

3.2. Immobilized Sema6A impedes growth from lumbosacral, but not thoracic or cervical DRG explants

The chemorepulsive effects of Sema6A have most often been identified through observations of growth cone collapse in response to soluble Sema6A-Fc fusion proteins (Suto et al., 2005; Suto et al., 2007; Xu et al., 2000). Because Sema6A is expressed as a transmembrane protein *in vivo*, we sought to investigate the effects of the protein in a more biomimetic, 3D presentation *in vitro*. The geometry of the micropattern was designed to maximize exposure of neurites to immobilized protein. Neurites from DRG explants grew robustly into the permissive agarose gel and were constrained by the restrictive PEG border. Consistent with our previous reports, confocal micrographs revealed neurite growth

throughout the 3D depth provided by the gels (data not shown). Growth was prominent at the interface of PEG and agarose (Curley and Moore, 2011), and some neurite growth into agarose could be seen infiltrating from this area.

Neurite growth was quantified from thresholded confocal image stacks of β III tubulin stained DRG constructs. Neurite avoidance of the channel containing immobilized protein compared to the channel containing no protein was measured as a guidance ratio calculated from the volumes of neurite growth in either channel. Neurite aversion to bound Sema6A was apparent and found to be dependent on DRG explant spinal level, with only lumbosacral neurites exhibiting chemorepulsion (Fig. 4). Significantly negative responses were only seen in lumbosacral DRG explants with values of -0.41 ± 0.20 and -0.33 ± 0.15 for 5 ng/mL and 20 ng/mL NGF respectively (Fig. 5). Neurite aversion was not manifested as turning at the border of bound Sema6A, but rather neurites appeared either to remain in place or grow extremely slowly upon entering the Sema6A region.

No response was observed in cervicothoracic or thoracic DRG explants (Fig. 4). Neurite extension at these spinal levels is apparent in the Sema6A region and of density and length comparable to the channel lacking Sema6A. Guidance ratios for thoracic and cervicothoracic DRG explants reflected no inhibitory effect of Sema6A (Fig. 5). Neurite growth in BSA controls also showed no significant preference for either channel (Fig. 4, 5). Differences in total neurite density between spinal levels were not observed for BSA or Sema6A conditions, suggesting that overall growth from different DRG types was not responsible for any differences in guidance ratio.

3.3. Sema6A chemorepulsion not reversed with uniform NGF concentration

We hypothesized that neurites of DRG explants cultured in elevated NGF concentrations may resist Sema6A repulsion, as has been shown for Sema3A inhibition in DRG (Ben-Zvi et al., 2008; Dontchev and Letourneau, 2002). To test this, the neurite avoidance assay was performed in the presence of both 5 ng/mL and 20 ng/mL NGF. Guidance ratios for both low and high concentrations of NGF indicated chemorepulsion at the lumbosacral region, with no significant difference between concentrations (Fig. 5). The lack of any uniform NGF effect on Sema6A chemorepulsion was surprising, and this point is elaborated upon further in the discussion.

3.4. Immobilized Ephrin-B3 does not influence DRG neurite growth, regardless of spinal level or NGF concentration

Ephrin-B3 is another transmembrane protein that has also been shown to be chemorepulsive to cortical neurites (Benson et al., 2005; Yokoyama et al., 2001), but we have not found any reports of Ephrin-B3 chemorepulsion in embryonic DRG explants. We tested immobilized Ephrin-B3 in the micropatterned neurite avoidance assay to compare with results of immobilized Sema6A. However, no appreciable repulsive response was observed in any of the DRG explants tested (Fig. 4, Fig. 5). The average concentration of Ephrin-B3 bound to agarose was 194 ± 40 nM. Channels with immobilized Ephrin-B3 had similar distances and densities of neurite ingrowth compared to channels lacking immobilized protein (Fig. 4). Growth ratios were comparable to those of BSA (Fig. 5). Neurite density again increased

with higher NGF concentrations, and no difference in total neurite outgrowth between spinal levels was observed for Ephrin-B3 conditions. The EphA4 receptor has been previously shown to regulate Ephrin-B3 chemorepulsion (Duffy et al., 2012), and antibody staining showed low levels of fluorescence across all DRG explant spinal levels with no significant differences in average values (Fig. 7 E–H).

3.5. NGF concentration gradient partially attenuates dose-dependent Sema6A chemorepulsion of lumbosacral DRG neurites

Increased background NGF levels did not improve the ability for neurites to overcome Sema6A repulsion, but we reasoned that NGF presented as a gradient may be able to attract neurite growth through immobilized Sema6A regions, partially counteracting or simply overriding the repulsive effect. Because we saw that lumbosacral DRG explants were the only DRG type to demonstrate a chemorepulsive response to Sema6A, we restricted the NGF gradient experiments to that spinal level. We also hypothesized that the concentration of immobilized Sema6A could play a role in the degree to which outgrowth would occur. Both low and high immobilized concentrations of Sema6A were tested, with values of 24 ± 9 and 146 ± 27 nM respectively. To this end, a soluble NGF gradient, approximately 1% slope and ranging between 0.1 nM and 1 nM maximum concentration, was maintained inside of the agarose channel by periodic addition of 40 nM NGF to a reservoir within the PEG border (Fig. 2). A comparable gradient of molecular weight-matched soluble casein was used as a control, as previously described by Rosoff, et al. (Rosoff et al., 2004).

From the representative qualitative images (Fig. 6 A) along with quantitative pixel counts, neurites showed an aversion to the Sema6A immobilized region in the presence of the control casein gradient, but were able to extend processes farther into Sema6A in the presence of the NGF gradient. The occurrence of growth in both channels is similar to 2D experiments demonstrating baseline radial DRG growth in all directions, with a statistical preference towards chemoattractants (Rosoff et al., 2004). With lower concentrations of Sema6A, additional neurite growth was apparent in the casein channel compared to higher Sema6A concentrations, and again, an increase in outgrowth was seen towards the NGF channel. Control constructs with immobilized BSA showed approximately equal maximum distances of outgrowth into the channels, with increased density towards the NGF gradient.

Guidance ratios incrementally increased depending upon the concentration of Sema6A (Fig. 6 B). Our control condition (BSA) had an average guidance ratio of 0.225 ± 0.046, representing a chemoattractive response to the soluble NGF gradient. When the concentration of bound Sema6A was raised to 24 nM (10% Sema6A), the guidance ratio increased to 0.365 ± 0.086, and the highest concentration of 146 nM (100% Sema6A) had the highest guidance ratio of 0.528 ± 0.090. Only the 100% Sema6A condition was significantly different from the other two conditions, but all conditions were statistically above a zero guidance condition.

3.6. Sema6A chemorepulsion of lumbosacral DRG explants correlates with Plexin A4 expression

In order to attempt to understand the increased response in lumbosacral DRG explants, we stained for the main receptor to Sema6A, Plexin A4. Although a multiplicity of receptors have been implicated in mediating the intracellular Sema6A response, Plexin A4 has been recognized to be primarily responsible for chemorepulsion in embryonic DRG explants (Haklai-Topper et al., 2010). Receptor influence is considered at length in the discussion. Immunostaining for Plexin A4 revealed a relatively low level of receptor expression confined mainly in the periphery of thoracic and cervicothoracic DRG explants (Fig. 7 A,B). In contrast, lumbosacral DRG explants expressed Plexin A4 throughout the volume of the explant, at a level approximately 42% higher ($p < 0.01$) than either thoracic or cervicothoracic expression (Fig. 7 C,D). There was no significant difference in mean fluorescence between thoracic and cervicothoracic DRG explants. These results correlated well with the observed spinal-level-dependent chemorepulsion of immobilized Sema6A suggesting that Plexin A4 expression level may mediate the inhibitory effect of Sema6A, though the basal level of expression in all explants reflects some uncertainty. This topic, and previously reported receptor expression data, is described at length in the discussion.

4. Discussion

Initial research using soluble growth cone collapse assays revealed much about semaphorins, but *in vitro* models were limited by a lack of biomimetic conditions. Xu et al. demonstrated the dimerization dependent chemorepulsive nature of Sema6A (Xu et al., 2000), while soluble experiments were also used to identify Plexin A4 as a direct Sema6A receptor (Suto et al., 2005). However, Sema6A is believed to function primarily as a transmembrane protein *in vivo*, and the differences in cellular interaction between soluble and immobilized molecules are significant and wide ranging (Ito, 2008). One previously published study did examine axon growth on Sema6A expressing COS cells, more closely mimicking *in vivo* conditions, though the *in vitro* model utilized 2D cell monolayers (Mauti et al., 2007). The method we used demonstrated the influence of the ectodomain portion of transmembrane ligands immobilized quantifiably in a 3D *in vitro* model, which may more accurately represent *in vivo* conditions, as compared to soluble application to neurons plated in 2D. We also demonstrated effectively that soluble protein gradients could be examined simultaneously within the same model.

Experimental results from our model showed a conditional chemorepulsive response to Sema6A, while no inhibitory interactions were seen with BSA controls or Ephrin-B3. Neurite density in channels containing immobilized BSA was comparable with that of the channel without immobilized protein. Neurites from lumbosacral DRG explants avoided the Sema6A bound channel in both 5 ng/mL and 20 ng/mL NGF conditions, as evident from β III tubulin staining and guidance ratio values (Fig. 4 and 5). Lumbosacral DRG explants displayed negative guidance ratios of −0.33 versus −0.41 when cultured in 20 ng/mL NGF compared to 5 ng/mL, relatively, but no significant inhibition of chemorepulsion was seen, as the difference was not statistically different. DRG neurites from other spinal levels were visualized growing through Sema6A, with no apparent repulsive interactions. Further

experimentation at the level of individual growth cones with a larger sample size may be required to confirm or rule out the possibility of an effect. Our findings are in line with some seemingly conflicting previous reports, which found apparent DRG neurite insensitivity to Sema6A, when cervical or unclear choice of DRG explants were used (Haklai-Topper et al., 2010; Xu et al., 2000), versus a clear Sema6A-mediated repulsion of lumbosacral DRG axons *in vitro* and regulation of dorsal root segregation *in vivo* (Mauti et al., 2007).

Initial experimental design included low (5 ng/mL) and high (20 ng/mL) NGF concentrations in order to test whether bath NGF concentration had a down-regulating effect on Sema6A repulsion, as previously seen with Semaphorin 3A (Dontchev and Letourneau, 2002; Tang et al., 2004; Tuttle and O'Leary, 1998). Surprisingly, our findings showed that guidance ratios of cultures with 20 ng/mL NGF were not significantly different than 5 ng/mL conditions (Fig. 5). We should point out that growth was never completely lacking in the Sema6A bound channels, and a prounounced and consistent concentration of neurites grew at the border of PEG and agarose. Some neurites entered the Sema6A-containing portion of the agarose, where growth appeared to slow significantly (Fig. 4). Additionally, neurites were observed to extend first at the interface between PEG and agarose (Fig. 4), as described previously (Curley and Moore, 2011). With increased incubation time, some neurites then infiltrated the gel peripherally from this border, potentially exaggerating this effect in low NGF conditions. While the interfacial growth was not included in the volume analysis and guidance ratio calculations, it is an aspect of our model system and/or the guidance ratio metric which will be addressed. The future use of an interpenetrating network of hydrogels or a single gel system should negate the existence of this border region. Still, our model served to clarify previously unknown effects of Sema6A and NGF which may be of benefit, and additional exploration of the more subtle aspects may be warranted. The effect of increased bath NGF appeared nuanced enough that a micro-scale investigation at the individual axon level would be required, while the experiments described here were better suited for population-level guidance experiments mimicking *in vivo* conditions.

Receptor expression mediated Sema6A chemorepulsion in DRG explants likely explains the haptotactic differences between DRG spinal levels. Plexin A4 is understood to be the main Sema6A receptor for embryonic DRG, and staining showed an increase in expression for lumbosacral DRG explants compared to thoracic and cervicothoracic levels (Fig. 7). High levels of Plexin A4 have been previously demonstrated in the lumbosacral region (Mauti et al., 2006) and in rat sciatic nerve (L4–L6) for DRG (Gutekunst et al., 2012). Plexin A2 has also been identified as a potential Sema6A suppressing receptor (Suto et al., 2007) and expression has been reported to be more prominent rostrally in DRG, with lumbosacral DRG showing only a subset of cells expressing the receptor (Mauti et al., 2006). Taken together, these data seem to correlate with differences in DRG explant responses to Sema6A.

Gradients of NGF showed an ability to overcome the chemorepulsive nature of Sema6A, and this phenomenon occurred in a manner dependent on the concentration of immobilized protein (Fig. 6). NGF is well known to be chemoattractive to sensory neurons, particularly when presented as a gradient (Gundersen and Barrett, 1979; Letourneau, 1978; Rosoff et al., 2004), and in our model empiric gradient profile experiments demonstrated predictable and

quantifiable diffusion patterns (Fig. 3). Guidance ratios increased with the concentration of Sema6A (0 for BSA, 23.8 and 146 nM), and analysis of the images suggested this result was dominated by a lack of neurite infiltration towards casein (Fig. 6 A–C). Guidance ratios seen for the BSA condition were comparable with similar ranges of NGF gradients previously reported (Rosoff et al., 2004), though higher in some cases, probably due to the confined growth conditions and increased incubation times (Fig. 6 D). Increased neurite growth overall was seen in the BSA condition, with a higher density of growth towards NGF. Growth did occur towards casein, a molecule which should demonstrate no guidance potential, but the nature of DRG neurites to grow radially, as well as the presence of minimal levels of NGF at the DRG itself may explain the occurrence of growth in both channels (Fig. 6 B,C). Additionally, we mentioned previously that some growth did occur in Sema6A, albeit in a stunted manner. However, the increase in neurite density and guidance ratio suggests a chemoattractive response towards NGF gradients. In the 100% Sema6A condition, and to a lesser extent in the 10% Sema6A condition, neurites appeared to be repelled by the Sema6A in the channel containing the casein gradient, while growing more readily into the gel towards the chemoattractive NGF (Fig. 6 A,B). It could be argued that this is not a guidance event, but rather some combination of increased axon stabilization and accelerated growth towards an NGF source. Nonetheless, when examined in the context of Sema6A repulsion and CNS injury models (Shim et al., 2012), it becomes clear that, whatever the mechanism, NGF gradients served to attract increased growth into an otherwise inhibitory region, with possible implications in regenerative strategies. As discussed above, the earlier findings that higher overall NGF concentration does not significantly decrease chemorepulsion of Sema6A seems to dispel the notion that NGF simply downregulates chemorepulsion. Instead, it appears that upregulation of growth by NGF gradients serves to overcome the chemorepulsion of Sema6A in a way absolute NGF concentration did not.

The lack of response of DRG explants to Ephrin-B3 at any spinal level represents an interesting finding, though we caution against strong conclusions (Fig. 4, 5). No guidance ratio at any spinal level was significantly different than BSA controls. Ephrin-B3 has previously been shown to be repulsive to axons of cortical neurons (Benson et al., 2005), as well as certain populations of thalamocortical axons (Takemoto et al., 2002). Duffy et al. reported that deletion of Ephrin-B3 from CNS myelin reduces inhibitory activity in adult DRG, suggesting that the protein does display chemorepulsive properties (Duffy et al., 2012). However, as previously reported, EphA4, the main receptor for Ephrin-B3, was not expressed in DRG at any embryonic stage (Eberhart et al., 2000). Antibody staining for EphA4 showed a similar trend, with extremely low fluorescence values for all DRG explants (Fig. 7 H). Changes in receptor expression and even function are common from embryonic to adult neurons, so it is possible that the embryonic stage of DRG explants we chose did not express sufficient levels of EphA4 receptor and was therefore not responsive to Ephrin-B3 (Fig. 7 E–G). Alternatively, the effective concentration of Ephrin-B3 may have been too low. Due to a gap in the literature, we found this negative result important to report.

Protein immobilization in our dual hydrogel constructs was demonstrated to be effective with spatial specificity throughout the length of the experiments (Fig. 2 C). Maleimide-thiol conjugation strategies have been utilized extensively in hydrogels; our use of the chemistry

in conjunction with a specifiable dual hydrogel system resulted in a highly useful *in vitro* model. The differences in binding concentration among proteins tested were likely due to differences in molecular weight and accessible free amines on each protein (Fig. 2). The largest molecule we examined, Sema6A, showed the lowest effective binding concentration, while BSA was immobilized at the highest concentration. Due to the differences in bound concentration, BSA does contain some inherent limitations as a control, but it was impossible to match molecular weight exactly. It is also important to point out that the bound concentration of protein is an average, with previously discussed localized changes in binding density throughout the depth of the gel (Horn-Ranney et al., 2013). This also likely influenced the concentration measurements themselves, as the fluorescent intensity values in bound agarose would involve a summation of heterogeneous concentrations as opposed to the homogenous nature of the standard curve, but likewise an average value is obtained for the bulk region. It is understood that Sema6A dimerization is required for receptor-mediated repulsion, so we chose to immobilize the Fc chimeric protein to the gel, but it is not currently known how gel conjugation might affect dimerization. Reducing the percentage of total CNBC-agarose in a 1% agarose gel effectively limited the availability of thiol groups, decreasing the bound concentration of Sema6A. It is also possible that decreasing the concentration of Sema6A may have also lowered the probability of dimerization.

5. Summary and conclusions

We have described a unique model system which may be the only one enabling simultaneous investigation of soluble and immobilized guidance cues within a 3D matrix in a specifiable geometry. We propose that our choice point approach represents a useful methodology to efficiently investigate the interplay of multiple receptor-ligand interactions governing morphogenetic processes. The ease with which individual proteins can be incorporated into our model allows for the examination of virtually any molecule of interest, both in soluble and immobilized form, or in combination. The findings that Sema6A chemorepulsion depends on DRG spinal level and that NGF presented as a gradient may overcome such repulsion helps clarify previous findings regarding sensory Sema6A repulsion and interactions with NGF. The model system we have described may be useful as a screening tool for the identification of ligand “cocktails” effective for guiding populations of neurons expressing various levels of guidance receptors. However, the model will not replace single-cell, mechanistic studies at the level of the growth cone needed to parse nuanced interactions of multiple receptor-ligand systems.

Acknowledgments

This research was funded in part by a grant from the NIH (R21-NS065374) and an NSF CAREER Award to MJM (CBET-1055990).

References

Ben-Zvi A, Ben-Gigi L, Yagil Z, Lerman O, Behar O. Semaphorin3A regulates axon growth independently of growth cone repulsion via modulation of TrkA signaling. Cellular signalling. 2008; 20:467–479. [PubMed: 18096366]

Benson MD, Romero MI, Lush ME, Lu QR, Henkemeyer M, Parada LF. Ephrin-B3 is a myelin-based inhibitor of neurite outgrowth. Proc Natl Acad Sci U S A. 2005; 102:10694–10699. [PubMed: 16020529]

Curley JL, Jennings SR, Moore MJ. Fabrication of Micropatterned Hydrogels for Neural Culture Systems using Dynamic Mask Projection Photolithography. J Vis Exp. 2011:e2636.

Curley JL, Moore MJ. Facile micropatterning of dual hydrogel systems for 3D models of neurite outgrowth. J Biomed Mater Res A. 2011; 99:532–543. [PubMed: 21936043]

Desai A, Kisaalita WS, Keith C, Wu ZZ. Human neuroblastoma (SH-SY5Y) cell culture and differentiation in 3-D collagen hydrogels for cell-based biosensing. Biosens Bioelectron. 2006; 21:1483–1492. [PubMed: 16084714]

Dontchev VD, Letourneau PC. Nerve growth factor and semaphorin 3A signaling pathways interact in regulating sensory neuronal growth cone motility. J Neurosci. 2002; 22:6659–6669. [PubMed: 12151545]

Duffy P, Wang X, Siegel CS, Tu N, Henkemeyer M, Cafferty WB, Strittmatter SM. Myelin-derived ephrinB3 restricts axonal regeneration and recovery after adult CNS injury. Proc Natl Acad Sci U S A. 2012; 109:5063–5068. [PubMed: 22411787]

Eberhart J, Swartz M, Koblar SA, Pasquale EB, Tanaka H, Krull CE. Expression of EphA4, ephrin-A2 and ephrin-A5 during axon outgrowth to the hindlimb indicates potential roles in pathfinding. Developmental neuroscience. 2000; 22:237–250. [PubMed: 10894987]

Gundersen RW, Barrett JN. Neuronal chemotaxis: chick dorsal-root axons turn toward high concentrations of nerve growth factor. Science. 1979; 206:1079–1080. [PubMed: 493992]

Gutekunst CA, Stewart EN, Franz CK, English AW, Gross RE. PlexinA4 distribution in the adult rat spinal cord and dorsal root ganglia. Journal of chemical neuroanatomy. 2012; 44:1–13. [PubMed: 22465808]

Haklai-Topper L, Mlechkovich G, Savariego D, Gokhman I, Yaron A. Cis interaction between Semaphorin6A and Plexin-A4 modulates the repulsive response to Sema6A. The EMBO journal. 2010; 29:2635–2645. [PubMed: 20606624]

Harel NY, Strittmatter SM. Can regenerating axons recapitulate developmental guidance during recovery from spinal cord injury? Nat Rev Neurosci. 2006; 7:603–616. [PubMed: 16858389]

Horn-Ranney EL, Curley JL, Catig GC, Huval RM, Moore MJ. Structural and molecular micropatterning of dual hydrogel constructs for neural growth models using photochemical strategies. Biomed Microdevices. 2013; 15:49–61. [PubMed: 22903647]

Irons HR, Cullen DK, Shapiro NP, Lambert NA, Lee RH, LaPlaca MC. Three-dimensional neural constructs: a novel platform for neurophysiological investigation. Journal of Neural Engineering. 2008; 5:333–341. [PubMed: 18756031]

Ito Y. Covalently immobilized biosignal molecule materials for tissue engineering. Soft matter. 2008; 4:46–56.

Lai Y, Cheng K, Kisaalita W. Three dimensional neuronal cell cultures more accurately model voltage gated calcium channel functionality in freshly dissected nerve tissue. PloS one. 2012; 7:e45074. [PubMed: 23049767]

Letourneau PC. Chemotactic Response of Nerve-Fiber Elongation to Nerve Growth-Factor. Developmental Biology. 1978; 66:183–196. [PubMed: 751835]

Mauti O, Domanitskaya E, Andermatt I, Sadhu R, Stoeckli ET. Semaphorin6A acts as a gate keeper between the central and the peripheral nervous system. Neural development. 2007; 2:28. [PubMed: 18088409]

Mauti O, Sadhu R, Gemayel J, Gesemann M, Stoeckli ET. Expression patterns of plexins and neuropilins are consistent with cooperative and separate functions during neural development. Bmc Dev Biol. 2006:6. [PubMed: 16503992]

McCormick AM, Leipzig ND. Neural regenerative strategies incorporating biomolecular axon guidance signals. Annals of biomedical engineering. 2012; 40:578–597. [PubMed: 22218702]

Moore DL, Goldberg JL. Four steps to optic nerve regeneration. Journal of neuro-ophthalmology : the official journal of the North American Neuro-Ophthalmology Society. 2010; 30:347–360. [PubMed: 21107123]

Rahman N, Purpura KA, Wylie RG, Zandstra PW, Shoichet MS. The use of vascular endothelial growth factor functionalized agarose to guide pluripotent stem cell aggregates toward blood progenitor cells. Biomaterials. 2010; 31:8262–8270. [PubMed: 20684984]

Romero MI, Rangappa N, Garry MG, Smith GM. Functional regeneration of chronically injured sensory afferents into adult spinal cord after neurotrophin gene therapy. J Neurosci. 2001; 21:8408–8416. [PubMed: 11606629]

Rosoff WJ, Urbach JS, Esrick MA, McAllister RG, Richards LJ, Goodhill GJ. A new chemotaxis assay shows the extreme sensitivity of axons to molecular gradients. Nature neuroscience. 2004; 7:678–682.

Roy J, Kennedy TE, Costantino S. Engineered cell culture substrates for axon guidance studies: moving beyond proof of concept. Lab Chip. 2013; 13:498–508. [PubMed: 23288417]

Runker AE, Little GE, Suto F, Fujisawa H, Mitchell KJ. Semaphorin-6A controls guidance of corticospinal tract axons at multiple choice points. Neural development. 2008; 3:34. [PubMed: 19063725]

Schmidt CE, Leach JB. Neural tissue engineering: Strategies for repair and regeneration. Annual Review of Biomedical Engineering. 2003; 5:293–347.

Shim SO, Cafferty WBJ, Schmidt EC, Kim BG, Fujisawa H, Strittmatter SM. PlexinA2 limits recovery from corticospinal axotomy by mediating oligodendrocyte-derived Sema6A growth inhibition. Molecular and Cellular Neuroscience. 2012; 50:193–200. [PubMed: 22564823]

Sofroniew MV, Howe CL, Mobley WC. Nerve growth factor signaling, neuroprotection, and neural repair. Annual review of neuroscience. 2001; 24:1217–1281.

Suto F, Ito K, Uemura M, Shimizu M, Shinkawa Y, Sanbo M, Shinoda T, Tsuboi M, Takashima S, Yagi T, Fujisawa H. Plexin-a4 mediates axon-repulsive activities of both secreted and transmembrane semaphorins and plays roles in nerve fiber guidance. J Neurosci. 2005; 25:3628–3637. [PubMed: 15814794]

Suto F, Tsuboi M, Kamiya H, Mizuno H, Kiyama Y, Komai S, Shimizu M, Sanbo M, Yagi T, Hiromi Y, Chedotal A, Mitchell KJ, Manabe T, Fujisawa H. Interactions between plexin-A2, plexin-A4, and semaphorin 6A control lamina-restricted projection of hippocampal mossy fibers. Neuron. 2007; 53:535–547. [PubMed: 17296555]

Takemoto M, Fukuda T, Sonoda R, Murakami F, Tanaka H, Yamamoto N. Ephrin-B3-EphA4 interactions regulate the growth of specific thalamocortical axon populations in vitro. The European journal of neuroscience. 2002; 16:1168–1172. [PubMed: 12383247]

Tang XQ, Heron P, Mashburn C, Smith GM. Targeting sensory axon regeneration in adult spinal cord. J Neurosci. 2007; 27:6068–6078. [PubMed: 17537979]

Tang XQ, Tanelian DL, Smith GM. Semaphorin3A inhibits nerve growth factor-induced sprouting of nociceptive afferents in adult rat spinal cord. J Neurosci. 2004; 24:819–827. [PubMed: 14749426]

Tuttle R, O'Leary DD. Neurotrophins rapidly modulate growth cone response to the axon guidance molecule, collapsin-1. Molecular and cellular neurosciences. 1998; 11:1–8. [PubMed: 9608528]

Wood MD, Hunter D, Mackinnon SE, Sakiyama-Elbert SE. Heparin-binding-affinity-based delivery systems releasing nerve growth factor enhance sciatic nerve regeneration. Journal of biomaterials science. Polymer edition. 2010; 21:771–787. [PubMed: 20482984]

Xu NJ, Henkemeyer M. Ephrin-B3 reverse signaling through Grb4 and cytoskeletal regulators mediates axon pruning. Nature neuroscience. 2009; 12:268–276.

Xu XM, Fisher DA, Zhou L, White FA, Ng S, Snider WD, Luo Y. The transmembrane protein semaphorin 6A repels embryonic sympathetic axons. J Neurosci. 2000; 20:2638–2648. [PubMed: 10729344]

Yokoyama N, Romero MI, Cowan CA, Galvan P, Helmbacher F, Charnay P, Parada LF, Henkemeyer M. Forward signaling mediated by ephrin-B3 prevents contralateral corticospinal axons from recrossing the spinal cord midline. Neuron. 2001; 29:85–97. [PubMed: 11182083]

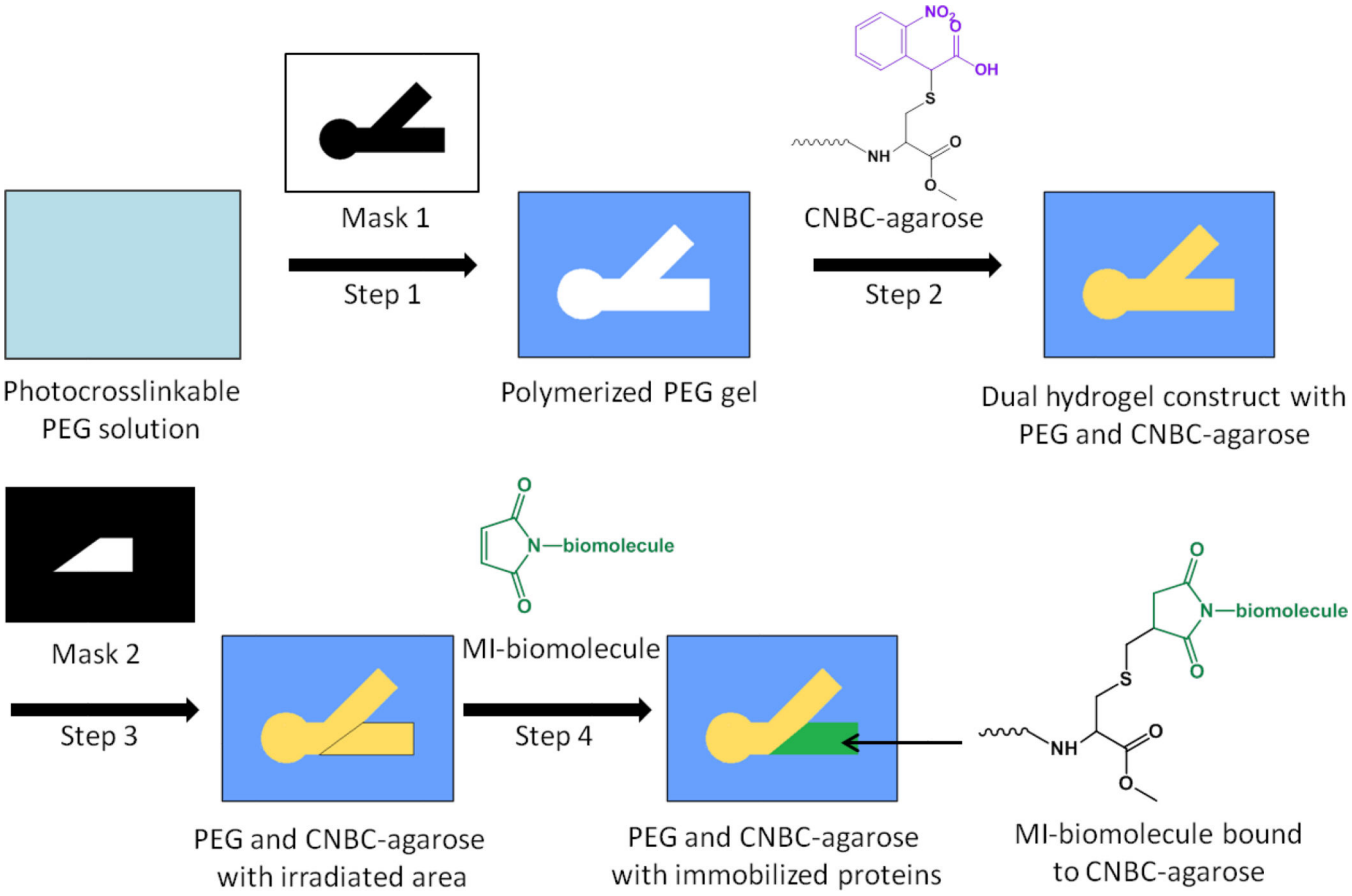

Figure 1.

Fabrication scheme for dual hydrogel constructs with 1% α-carboxy-2-nitrobenzyl cysteine agarose (CNBC-agarose) and immobilized cues. Step 1: A cell culture insert is filled with photocrosslinkable PEG solution. Using Mask 1, PEG solution is crosslinked via UV irradiation and uncrosslinked PEG is removed. Step 2: The PEG molds are filled with CNBC-agarose solution and crosslinked at 4° C. The photocleavable moiety on CNBC-agarose (purple) cages the thiol on the cysteine. Step 3: After gelation, CNBC-agarose is irradiated with UV using Mask 2. Irradiation uncages the thiol moiety on CNBC-agarose, providing a binding site for maleimide-activated (MI) biomolecules. Step 4: Inserts are soaked in MI-biomolecule solution tagged with fluorescent markers, resulting in a region of immobilized MI-biomolecules in CNBC-agarose.

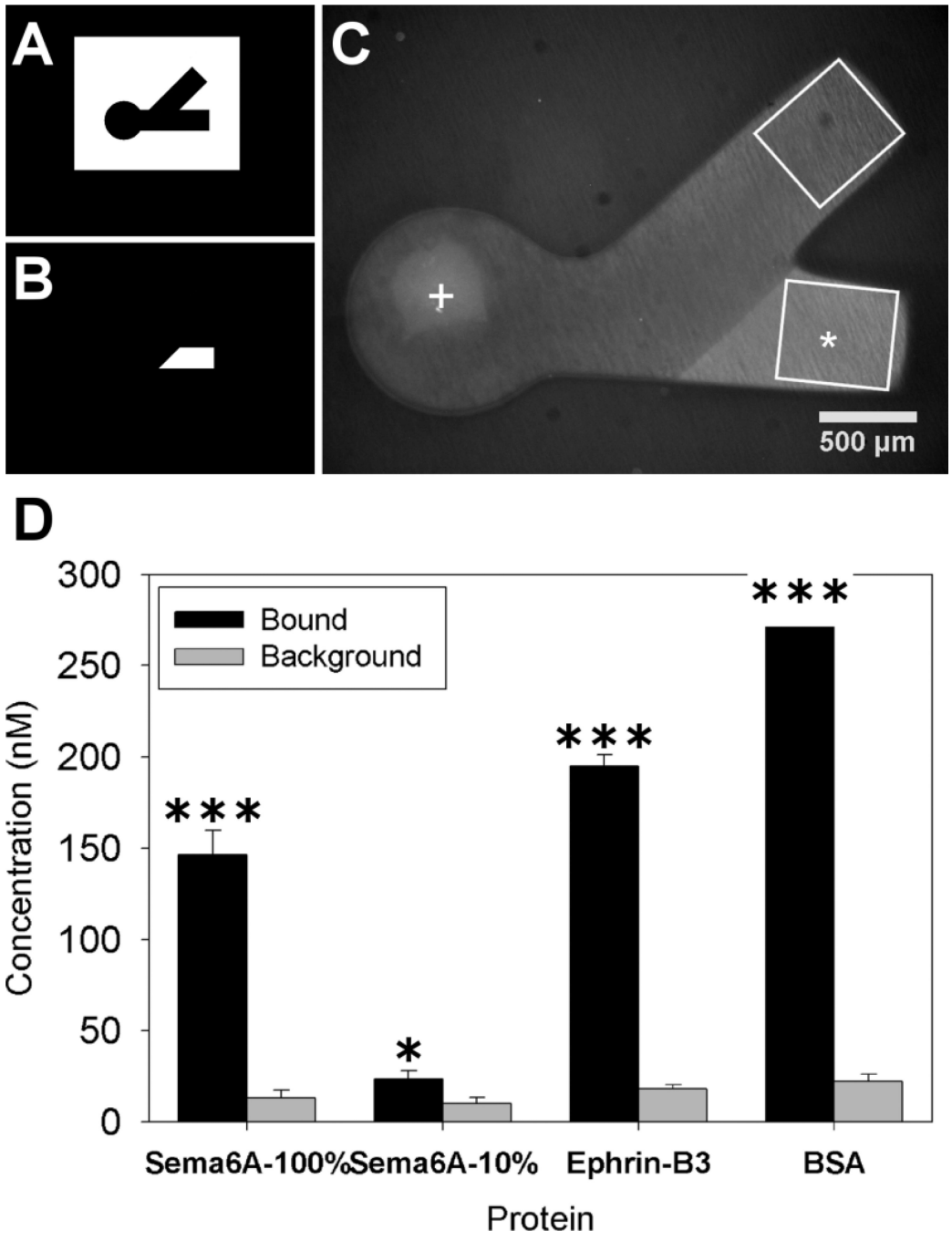

Figure 2.

Polymerization and protein binding for immobilized choice point models. Photomasks used for polymerization of PEG (**A**) and for spatial immobilization of proteins (**B**). Dual hydrogel construct used for immobilized protein experiments (**C**) with protein binding region indicated with *(Sema6A), white box approximating immunofluorescent ROI and + marks DRG explant location. The average concentration of immobilized protein in agarose (**D**) for the irradiated channel (bound) along with the average amount of protein seen in the non-irradiated channel (background) was plotted for each of the separate proteins used (n=10).

The amount bound in irradiated regions was significantly higher than background fluorescence in non-irradiated regions for all bound proteins (student's t-test, * $p < 0.05$ and *** $p < 0.001$).

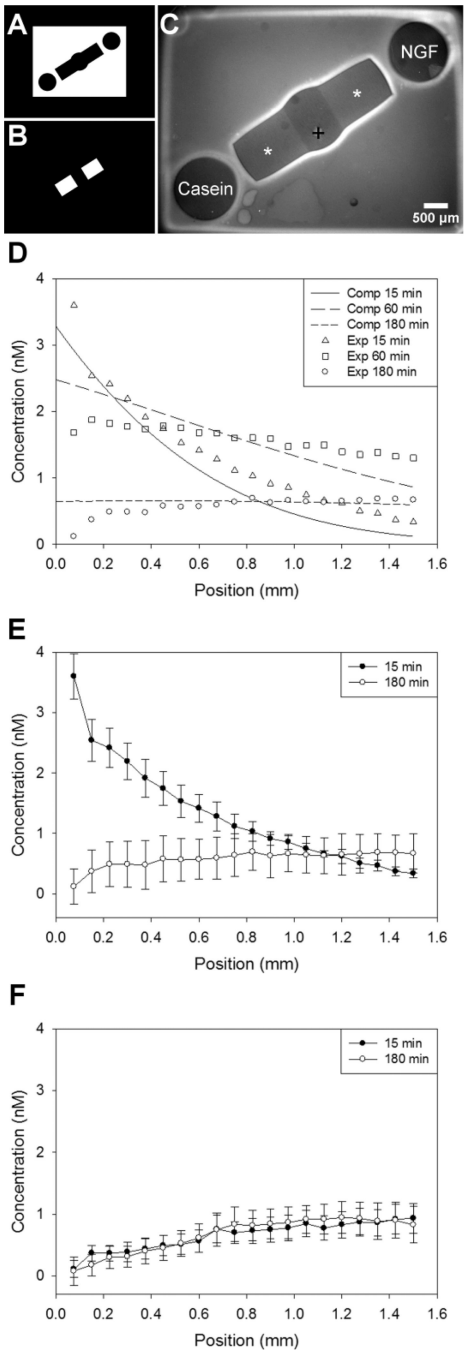

Figure 3.

Polymerization and protein diffusion for gradient choice point models. Photomasks used for polymerization of PEG (**A**) and for spatial immobilization of proteins (**B**). Dual hydrogel construct used for soluble gradient experiments (**C**) with protein binding region indicated with *(BSA), and + marks DRG explant location. **D**, Computational and experimental concentration profiles of soluble NGF diffusion through CNBC-agarose regions, demonstrating that the initial gradient formation and behavior through time was as expected. **E**, Experimental concentration profiles demonstrating gradient upon establishment and

before refilling. **F**, NGF concentration profile in opposite channel was minimal and in the opposite direction. Concentration values were determined along center of channel with position 0.0 mm corresponding to the end of the channel nearest the soluble NGF reservoir (D,E) or soluble casein reservoir (F); DRG located at ~1.5 mm (n=3).

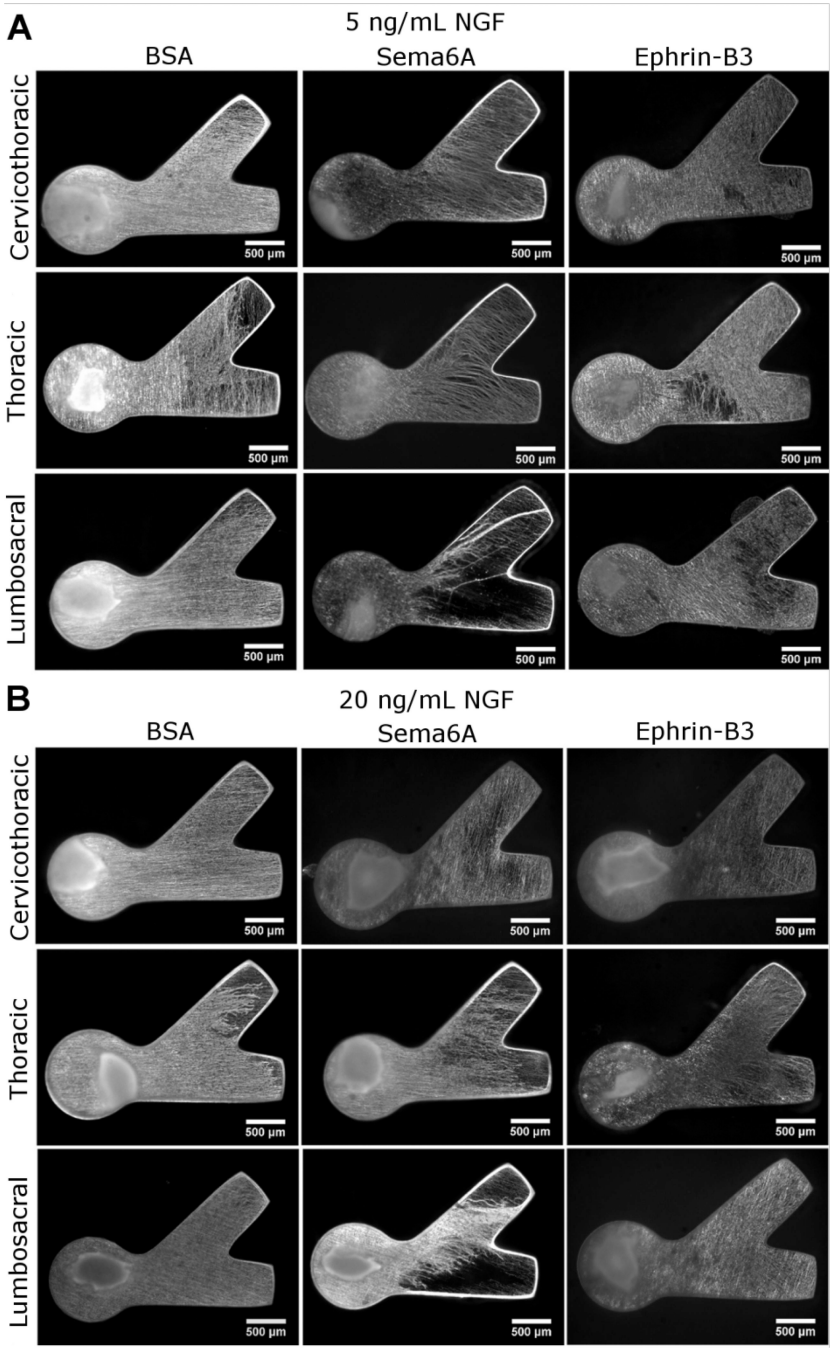

Figure 4.

Neurite responses to protein binding. βIII tubulin stained neurite growth inside CNBC-agarose with immobilized protein in lower channel. Labels indicate type of protein immobilized as well as DRG spinal regions tested. Culture conditions of 5 ng/mL NGF (A) or 20 ng/mL NGF (B) were used. Neurites only exhibited a chemorepulsive response to Sema6A at the lumbosacral region, avoiding the channel containing immobilized Sema6A. Equal volumes of growth were apparent in channels containing immobilized protein and channels lacking bound for all other proteins and spinal levels.

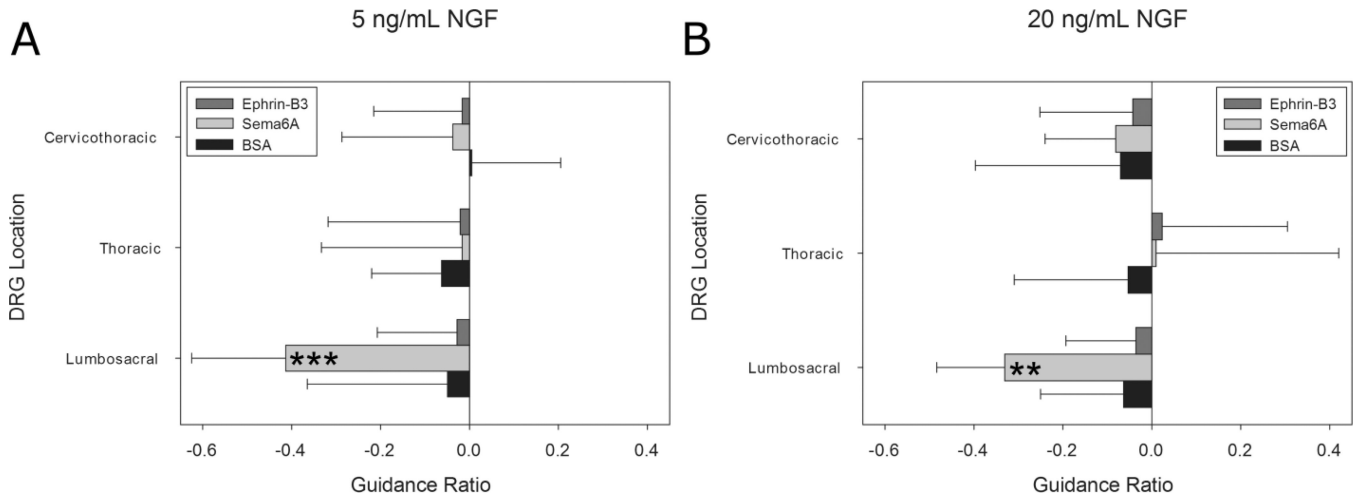

Figure 5.

Immobilized effects of Ephrin-B3, Sema6A and BSA on DRG explant outgrowth from three distinct spinal levels. Negative guidance ratio values represent growth inhibition in region containing immobilized proteins. **A**, only Sema6A at the lumbosacral region showed a chemorepulsive response with a homogenous level of 5 ng/mL NGF (***$p < 0.001$). All other spinal levels and proteins displayed near zero guidance ratios. **B**, At higher NGF concentrations, only Sema6A at the lumbosacral region demonstrated chemorepulsion (**$p<0.01$). No statistically significant change in the average guidance ratio was apparent compared to 5 ng/mL NGF. For all conditions n=12. Error bars represent standard deviation. Significance determined with one-way ANOVA performed separately followed by the Games-Howell post-hoc analysis.

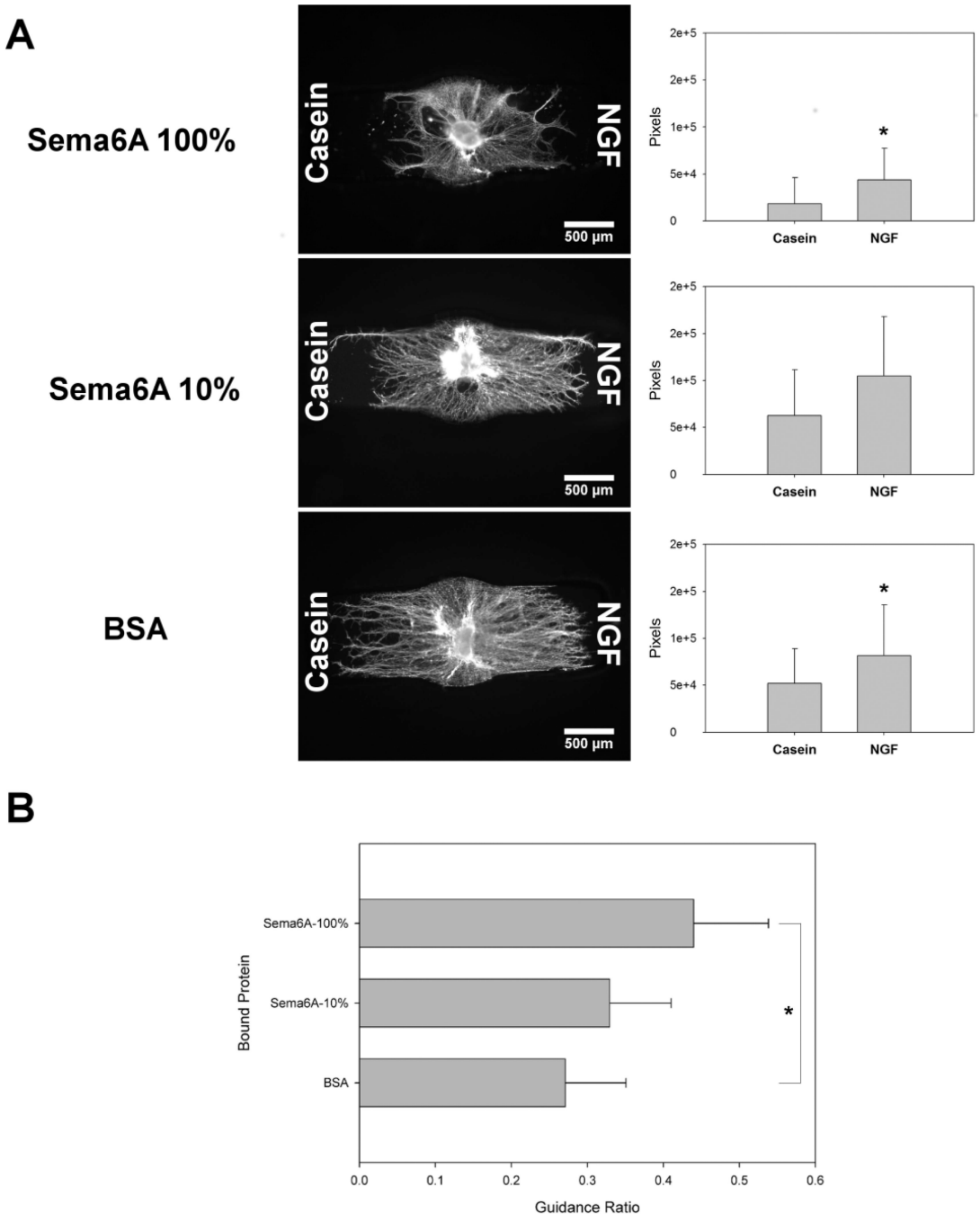

Figure 6.

Effect of soluble gradients of casein (left channel) and NGF (right channel), in conjunction with immobilized Sema6A (high and low concentrations) and BSA, on DRG explant outgrowth. Each bound protein is immobilized on both sides of channel, and positive guidance ratios represent increased growth through bound protein toward NGF gradient, compared to control casein gradient. **A** Left, Sema6A immobilized with 100% CNBC-A showed sparse neurite growth in the casein gradient channel, with many neurites crowding the border of the bound region, but increased growth towards the NGF gradient. Right,

separate pixel counts for β III tubulin positive neurites in both Casein and NGF channels. **B**, Sema6A immobilized with 10% CNBC-A demonstrated increased growth into the casein region, but still neurite density and overall length was higher towards NGF. **C**, BSA immobilized channels did not seem to show a difference in overall length of neurites, but increased density was apparent towards NGF. **D**, Guidance ratios corroborated the preference for neurite growth towards the NGF gradient channel, with the greatest difference from control seen with Sema6A-100% and the least in BSA (n=12). One-way ANOVA performed separately followed by the Games-Howell post-hoc analysis (*$p < 0.05$).

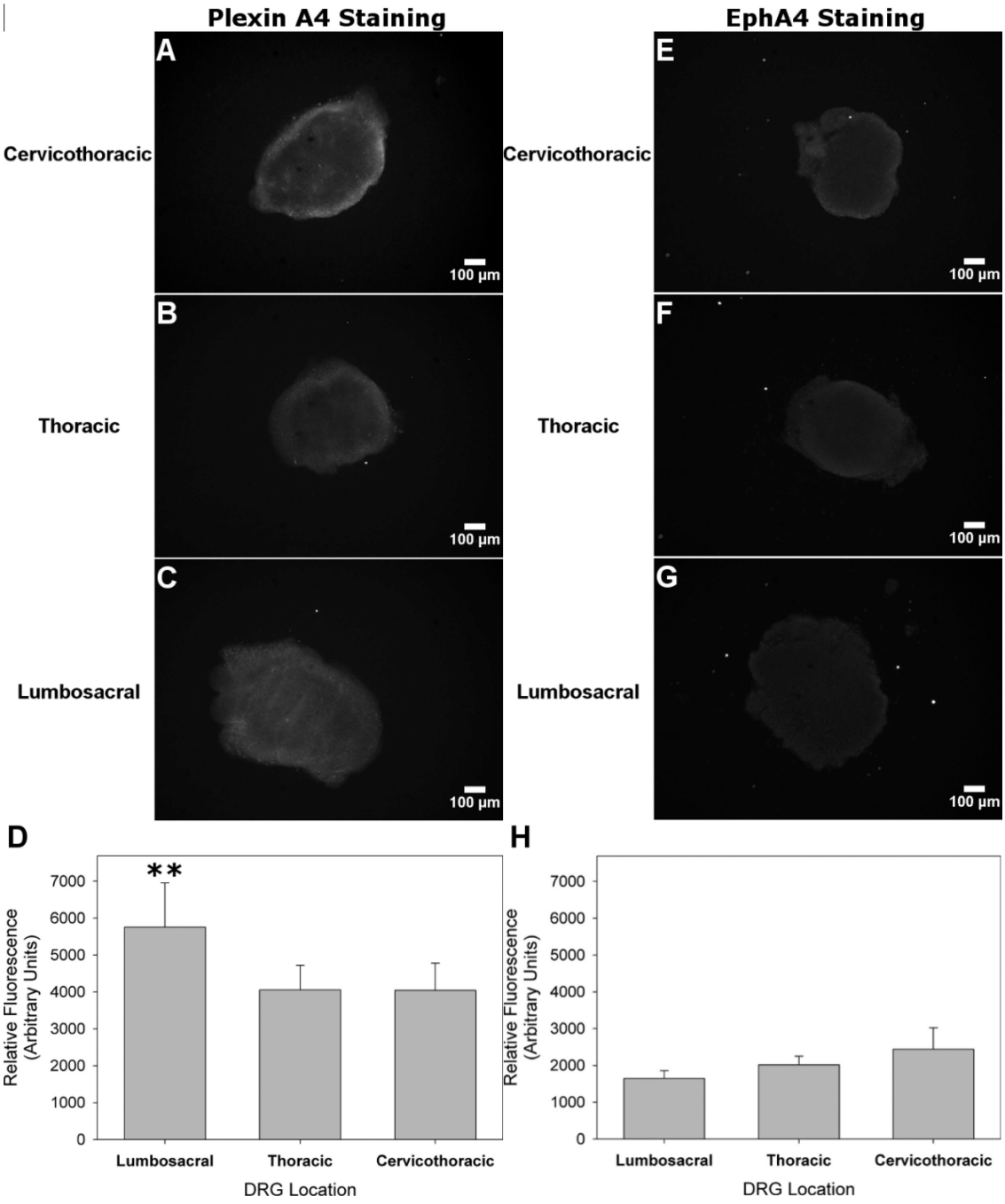

Figure 7.

Differences in levels for Plexin A4 and EphA4 antibody staining between spinal levels. **A,B,** Plexin A4 receptor expression visualized through antibody fluorescence was evident in the peripheral region of cervicothoracic and thoracic DRG explants. **C,** Receptor expression was observed in the periphery as well as the central region of lumbosacral DRG explants. **D,** Relative fluorescence units plotted across DRG spinal level demonstrated increase mean values in lumbosacral compared to thoracic or cervicothoracic DRG explants. **E–G,** EphA4 was faintly visible in the peripheral regions of all three spinal levels. **H,** Relative

fluorescence units were all less than Plexin A4 levels and were not significantly different among spinal levels. One-way ANOVA performed separately followed by the Games-Howell post-hoc analysis (n=6, **$p < 0.01$).